JOURNAL OF MATERIALS SCIENCE 14 (1979) 953–960

# Plastic deformation by crazing in polycarbonate

M. KITAGAWA
*Department of Mechanical Engineering, Faculty of Technology, Kanazawa University, Kanazawa, Japan*

M. KAWAGOE
*Department of Mechanical Engineering, Toyama Technical College, Toyama, Japan*

On the basis of the data of craze behaviour under static tension, the deformation curves followed by continuous initiation and growth of crazes are plotted for a variety of testing conditions, such as constant stress, constant strain-rate and constant strain tensions applying the Johnston–Gilman theory for dislocations. Experimentally determined values of the density and growth rate of crazes, which are regulated in accordance with a simple rate theory, are used for the calculations. Comparison of the theory with the experimental results is favourable except for the results of high strain-rate tension and stress relaxation. The application of the dislocation analogue approach to the craze deformation kinetics was found to be valuable.

## 1. Introduction

High polymer solids may craze and crack when subjected to stresses in some environments. The yield point followed by continuous initiation and growth of crazes is much lower than the shear yield point without crazing. The strain caused by crazing, (craze strain) increases with increasing craze density which (i.e. the the number of crazes per unit volume or surface area). Thus, the initiation and growth of crazes play an important role in the deformation kinetics of polymer solids in a different way to shear yielding. Therefore, theoretical analysis of the deformation behaviour due to crazing is of considerable interest.

Hoare and Hull [1], and Brown [2] have suggested, on the basis of a dislocation analogue, that the strain increase caused by crazing is expressed as function of the density, growth rate and thickness of craze. Subsequently, applying the Johnston–Gilman theory [3] of dynamic yielding of crystalline solids, Brown [4] has calculated the stress–strain curves followed by crazing, and has shown that the calculated curves agree with the experimental ones qualitatively, but not quantitatively. This quantitative disagreement may arise partly from the fact that the experimental values used for the calculation are not necessarily valid for craze density on a physical basis. He assumed that the craze density was independent of testing time. As demonstrated by Argon and Hannoosh [5], however, the craze density for a given applied stress increases with time and gradually approaches a saturation density. Therefore, a partial improvement of the calculation is needed.

It is the purpose of this paper to estimate theoretically from the data of craze behaviour under static tension the stress–strain relations followed by crazing for a variety of testing conditions such as creep, constant strain-rate tension and stress relaxation. Such an estimation will require the investigation of craze density and growth rate under static tension. A theoretical model of craze behaviour under static tension has been proposed by Argon and Hannoosh [5], and Argon and Salama [6]. However, their functional forms presented are complex, and not suitable for the calculations to be discussed here. Hence, craze behaviour, measured under static tension, is regulated in accordance with a simple rate theory, and the data will be used to calculate deformation kinetics. The theoretical deformation curves obtained are compared with the experimental results obtained from a polycarbonate plate under the action of a crazing agent, kerosene.

## 2. Experimental procedure

The material used was commercially available polycarbonate (PC) plate 1 mm thick (Takiron plate, Takiron Co, Japan). Dumb-bell shaped specimens (gauge part 10 mm x 20 mm) were cut from it, and then annealed for 1 h at 120° C and cooled in an oven to remove residual strain.

In order to observe the craze behaviour necessary for the theoretical calculation, static tensile tests were performed with a constant-load type testing machine constructed for this experiment. Five applied stresses between 3.5 and 4.5 kg mm$^{-2}$ were chosen, and five specimens were tested at each stress level. The dependence of the density and length of craze on time was determined from photographs taken through a low-power optical microscope at reasonable intervals without stopping the test. To prevent the nucleation of crazes from the side edges of the specimen surfaces, the edges were thinly covered by glue.

Constant stress or creep tests were also performed using the above method, creep elongation being measured by a clip gauge fastened between the testing jigs. For constant strain-rate tension and stress relaxation tests, an Instron-type tensile testing machine was used. Load–elongation curves during the tests were traced on an $X$–$Y$ recorder.

All the tests were carried out at room temperature (20 ± 1° C) under the action of a crazing agent, kerosene.

## 3. Experimental results

### 3.1. Density and growth rate of craze under static tension

Experimentally measured densities of craze as a function of time are shown in Fig. 1, where the solid surves are drawn on the basis of a theoretical model to be discussed later. Since the measured data were considerably dispersed for every specimen tested, the mean values were plotted in the figure. Examination of these data shows that for a given applied stress, the craze density initially increases with time but then gradually approaches a saturation density, and the saturation density increases with increasing applied stress. This trend is very similar to that observed by Argon and Hannoosh [5]. On the other hand, Narisawa and Kondo [7] have indicated, using the statistical observation on the dispersions of craze nucleation time, that its distribution function is a monotonically decreasing fucntion of time. This means

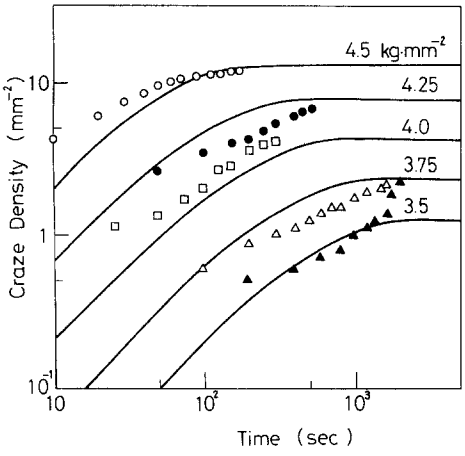


*Figure 1* Comparison of theoretical (———) and experimental variations of craze densities with time at different applied stresses.

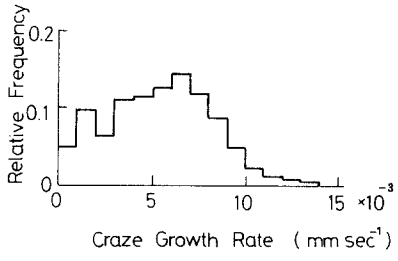


*Figure 2* Histogram of craze growth rate at an applied stress of 4.5 kg mm$^{-2}$.

that the frequencies of nucleation of new crazes decrease with time, and therefore is consistent with the present results.

A large number of measurements were made of craze length as a function of time at different stress levels. The length of craze varied linearly with time during the period of the test. The slopes of the growth curves for individual crazes, i.e. the rates of craze growth, showed large variations even on the same specimen. This is evident in Fig. 2, which shows an example of a frequency histogram of the growth rates of several hundred crazes which appeared on five specimens tested at an applied stress of 4.5 kg mm$^{-2}$. This dispersion, which probably arises partly from a slight bending of the specimen and partly from the essential statistical behaviour of crazes, may be important in understanding the statistical distribution of craze length at a given time. This statistical aspect will be reported elsewhere in detail [8]. As this paper is concerned with the average deformation behaviour, the mean growth rates are obtained from such figures as a function of applied stress.

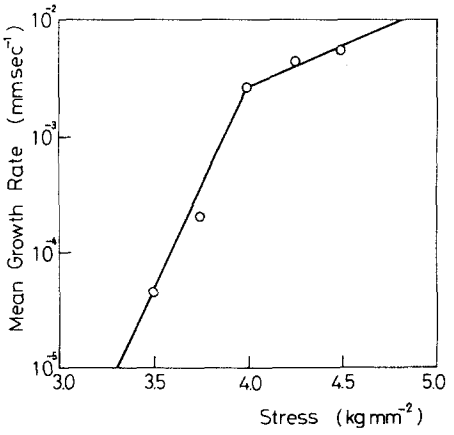


*Figure 3* Effect of applied stress on mean growth rate under static tension. The solid line drawn empirically is used for the theoretical calculations.

The results are shown in Fig. 3, where the solid line drawn empirically is used for the calculations discussed later.

## 3.2. Deformation curves

Experimental creep strain curves are shown as a function of time by the dotted lines in Fig. 4, where the solid curves are theoretical. Although the experimental curves for a given applied stress are fairly dispersed, the tendencies are very similar. The creep strain gradually increases with time during the initial stage and accelerates to a fracture strain at the final stage. The creep strain (total strain minus initial elastic strain) tested without a crazing agent was very small compared with that tested under kerosene. The increase in creep strain under kerosene may, therefore, be regarded as consisting of only craze strain. The creep fracture surfaces consisted of three typical regions, i.e. delayed fracture from craze crack, fast fracture with a smooth surface, and fast fracture with rough or so-called mackerel marks. The delayed crack growth from the crazed matter was found to be a precursor of final fracture. Thus, in order to establish a craze fracture criterion, a precise description of the craze creep strain will be required.

Experimental stress–strain curves tested at

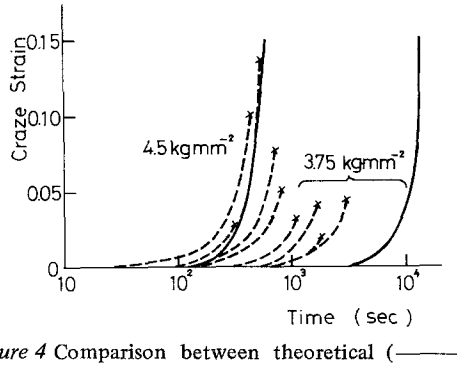


*Figure 4* Comparison between theoretical (———) and experimental (– – –) creep strains.

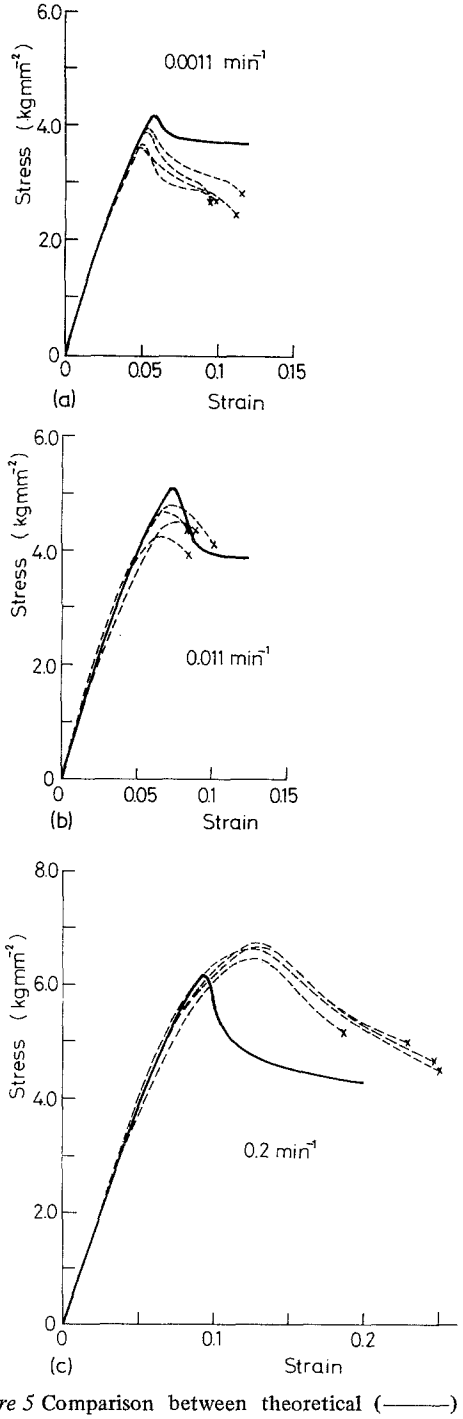


*Figure 5* Comparison between theoretical (———) and experimental (– – –) stress–strain curves at different strain-rates in simple tension.

three different strain rates in simple tension are shown by the dotted lines in Fig. 5. It could be observed by the naked eye that numerous crazes formed in the neighbourhood of the yield point, and shear bands peculiar to shield yielding did not appear. Furthermore, the dependence of the yield point on strain-rate was found to be considerably higher than that of the shear yield point (see Fig. 7). These observations may provide an important piece of evidence that the yielding is attributed to crazing, as pointed out by Brown. The yielding is called craze or normal yielding.

At lower stress levels during the test, few crazes were observed on the specimen surfaces. The elastic modulus, therefore, is not so affected by crazing and nearly equal to that tested in air, until the applied stress reaches a certain stress level. In excess of that stress, the craze density suddenly began to increase with increasing applied stress and the modulus gradually become lower than that in air. At relatively high strain rates, numerous *short* crazes were observed near the yield point, as such crazes have only a short time-interval in which to grow because of the high test speed, and because they interact due to the high craze density. The reverse is true for relatively low strain rates. After craze yielding, the stress decreases with increasing strain, and fracture occurs. Fracture strain or stress depends on strain-rate, probably because fracture has a close connection with the density and length of craze at the stage where fracture occurs.

Experimental stress relaxation curves are shown by the dotted lines in Fig. 6, where the solid curve is theoretical. At the beginning of the test, the specimens was subjected to a strain corresponding

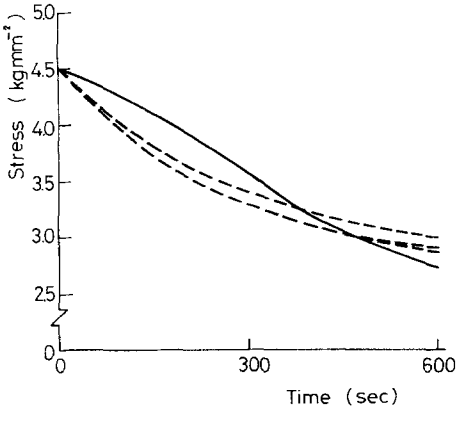


*Figure 6* Comparison between theoretical (——) and experimental (– – –) stress relaxation curves.

to an applied stress of $4.5\,\mathrm{kg\,mm^{-2}}$ in simple tension, and were then wet with kerosene as soon as possible. Crazes nucleated immediately on the specimen surfaces, and the relaxation of the initial applied stress occurs. The amount of stress relaxation in air was found to be smaller than that under kerosene.

## 4. Discussion

### 4.1. Craze behaviour under static tension

The purpose of this section is to derive, on the basis of a rate theory, functional forms of craze density and growth rate for an applied stress and time, which will then be used for calculating the theoretical deformation curves. The application of rate theory in a general form to the craze nucleation and growth processes does not require a specific molecular mechanism.

Let $\Delta G$ be the height of the free energy barrier required for craze nucleation. When a stress is applied, the barrier is biased in favour of craze nucleation by an amount $E(\sigma)$, strain energy input by a normal stress. The form of $E(\sigma)$ is usually written as $E(\sigma) = \alpha\sigma$, $\alpha$ being the activation volume. Thus the height of the barrier changes from $\Delta G$ to $\Delta G - \alpha\sigma$. In equilibrium, according to Boltzmann statistics, the fraction of craze particles per unit volume, $\rho_0$ with respect to the total number of craze nucleation sites per unit volume, $\rho^*$, is

$$\rho_0/\rho^* = \exp\left(-\frac{\Delta G - \alpha\sigma}{kT}\right), \qquad (1)$$

where $k$ is Boltzmann's constant and $T$ is the absolute temperature. $\rho_0$ corresponds to a craze saturation density. Let $\rho$ be the number of crazes per unit volume at a certain time $t$. The net rate of increase in $\rho$ may be proportional to the product of the rate constant, $m$, and the number of sites capable of craze nucleation, $\rho_0 - \rho$, and therefore can be described by

$$\frac{\mathrm{d}\rho}{\mathrm{d}t} = m(\rho_0 - \rho), \qquad (2)$$

where $\mathrm{d}\rho/\mathrm{d}t$ is the craze nucleation rate. According to the absolute reaction rate theory, the rate constant $m$ can be expressed as

$$m = A\frac{kT}{h}\exp\left(-\frac{\Delta G - \alpha\sigma}{kT}\right), \qquad (3)$$

where $h$ is Planck's constant and $A$ a factor of the

order of 1.0. Solving Equation 2 with the boundary condition $\rho = \rho_0$ at $t = \infty$ results in Equation 4 for the prediction of the time and stress-dependence of craze density.

$$\rho = \rho_0 [1 - \exp(-mt)]. \quad (4)$$

Equation 4 implies that the craze density initially increases with time and gradually approaches a saturation density dependent on the applied stress, and therefore qualitatively agrees with the experimental data. The solid curves in Fig. 1 show Equation 4 with the constants given in Equation 5. Here, the number of crazes per unit surface area is adopted in place of the number of per unit volume.

$$\begin{aligned} \rho_0 &= 3.6 \times 10^{-4} \exp(2.35\sigma) \\ m &= 4.0 \times 10^{-7} \exp(2.35\sigma) \end{aligned} \quad (5)$$

The units of $\rho_0$, $m$ and $\sigma$ used in Equation 5 are $cm^{-2}$, $sec^{-1}$ and $kg\,mm^{-2}$, respectively, The calculated curves for all applied stresses agree well with the experimental results. If $A$ is set equal to 1.0 in Equation 3, the constants $\Delta G$ and $\alpha$ are determined from Equation 5 to be $26\,kcal\,mol^{-1}$ and $1.0 \times 10^{-21}\,cm^3$, respectively. These values are considered to be reasonable in comparison with those obtained by Narisawa and Kondo [7].

A craze growth rate function with respect to the applied stress is determined from Fig. 3. A plot of log mean growth rate, $v$ versus applied stress, $\sigma$, is linear. Hence, the growth rate can be described by

$$v = v_0 \exp(B\sigma), \quad (6)$$

where $v_0$ and $B$ are constants. However, the deviation from the line drawn for the low stress range is observed at a high stress level. Strong interaction between crazes, which probably arise from the high craze density, may cause this deviation, as mentioned by Argon and Salama [6]. For the calculation shown in Section 4.2, the following values were, therefore, used; $v_0 = 4.03 \times 10^{-17}\,mm\,sec^{-1}$ and $B = 7.95\,mm^2\,kg^{-1}$ for the stress range lower than $4.0\,kg\,mm^{-2}$. and $v_0 = 3.84 \times 10^{-6}\,mm\,sec^{-1}$ and $B = 1.63\,mm^2\,kg^{-1}$ for the stress range higher than $4.0\,kg\,mm^{-2}$.

## 4.2. Theoretical calculation of deformation curves

The theory assumes that only elastic strain, $\epsilon_E$, and craze strain, $\epsilon_c$, occur in the specimen. Since the stiffness of a testing machine is considered to be very high, the total strain, $\epsilon$, is given by

$$\epsilon = \epsilon_E + \epsilon_c. \quad (7)$$

The elastic strain is given by

$$\epsilon_E = \sigma/M, \quad (8)$$

where $\sigma$ is the applied stress and $M$ is the elastic modulus of the material. According to the dislocation analogue, the strain caused by crazing has the following form [2].

$$\epsilon_c = \rho b a/z \quad (9)$$

where $z$ is the specimen thickness, $b$ is the opening displacement of the craze, $\rho$ is the number of crazes per unit surface area and $a$ is the craze area perpendicular to the tensile direction. If the change in $\rho$ with $t$ is very small, the craze strain-rate, $\dot{\epsilon}_c$, is written as

$$\dot{\epsilon}_c = \rho b \dot{a}/z, \quad (10)$$

where $\dot{a}$ is the extension rate of the craze area. On the basis of Equation 10, Brown [4] has calculated the stress–strain curves of polychlorotrifluoroethylene in simple tension. In this paper, however, we start with Equation 9 when estimating the plastic craze strain.

The pioneering experiments of Bessonov and Kuvshinsky [9] have revealed that the craze thickness increases with craze length. Thus, the craze thickness, $b$, is a function of the length of craze. Furthermore, crazes may grow also towards the direction perpendicular to the specimen surface. However, exact data expressing such craze behaviour have not been published. Therefore, the following assumptions are used;

$$\begin{aligned} a &= fl^2 \\ b &= gl \end{aligned} \quad (11)$$

where $l$ is the craze length measured on the specimen surface, and $f$ and $g$ are the shape factors. The experiments of Bessonov and Kuvshinsky show that the shape factor $g$ is about $2.5 \times 10^{-3}$. If the craze plane is semi-elliptical, and $f$ is 0.16, the craze length along the short axis of the ellipse is about $0.1 \times l$. This is comparable with the experimental result of Williams and Marshall [10].

Equation 9 may now be written as

$$\epsilon_c = K\rho l^3/z, \quad (12)$$

where $K$ is again the shape factor, i.e. $fg$. Although the factor $K$ may be dependent on applied stress, here it is assumed to be constant over the entire stress range. For the calculations discussed below, $K = fg = 2.5 \times 10^{-3} \times 0.16 = 4.0 \times 10^{-4}$ was used.

First, we consider creep deformation. The number of crazes $\Delta\rho$, which nucleate during an infinitesimal time interval from $\tau$ to $\tau + \Delta\tau$ is obtained from Equation 4 to be

$$\Delta\rho = m\rho_0 \exp(-m\tau)\Delta\tau. \quad (13)$$

At a certain time $t$ $(t > \tau)$, these crazes cause a strain increase expressed by

$$\Delta\epsilon_c = Kz^{-1}m\rho_0 \exp(-m\tau)[v(t-\tau) + l_0]^3 \Delta\tau, \quad (14)$$

where $v$ is the average craze growth rate for a given stress and $l_0$ is the initial craze length. Summing these strain increases leads to the total craze strain given by

$$\epsilon_c = \int_0^t Kz^{-1}m\rho_0 \exp(-m\tau)[v(t-\tau) + l_0]^3 \mathrm{d}\tau. \quad (15)$$

Elementary integration leads to

$$\epsilon_c = Kz^{-1}\rho_0 m^{-3}[x^3(y^3 - e^{-mt}) - 3vx^2(y^2 - e^{-mt}) + 6v^2x(y - e^{-mt}) - 6v^3(1 - e^{-mt})], \quad (16)$$

where $x = ml_0$ and $y = (v/l_0)t + 1$. The numerically calculated results of Equation 15 with the constants given in Equations 5 and 6, shown by the dotted curves, agree fairly well with the experimental data.

It is interesting to note that the computed values of Equation 15 can be numerically approximated by

$$\epsilon_c = D \exp(\beta\sigma)t^n, \quad (17)$$

where $D$, $\beta$ and $n$ are the constants. The value of $n$ is equal to 3.4 for the entire stress ranges, but the value of $\beta$ is different at each applied stress level, i.e. $\beta = 8.35$ at the high stress range and $\beta = 27.0$ at the low stress range. This difference in $\beta$ is attributed to the use of two different experimental expressions of $v$. Equation 17 is identical to the commonly used creep equation similar to the so-called Nutting equation.

Next, we consider the stress–strain curves under constant strain-rate tension. The important difference from the case of creep is that here the applied stress is a function of time. The density of crazes which nucleate during an infinitesimal time interval, $\Delta\tau$ is obtained by putting $\tau = 0$ in Equation 4 equal to $\rho_0 m\Delta\tau$. Crazes which nucleate at $\tau$ grow to $\int_\tau^t v(\sigma)\mathrm{d}\eta$ at a certain time, $\eta$ being the time. Then the craze strain at $t$ can be described by

$$\epsilon_c = Kz^{-1}\int_0^t \rho_0(\sigma)m(\sigma)\left[\int_\tau^t v(\sigma)\mathrm{d}\eta + l_0\right]^3 \mathrm{d}\tau. \quad (18)$$

The equation governing the stress–strain relation is obtained by combining Equations 7 and 18 to give

$$\dot{\epsilon}t = \sigma/M + Kz^{-1}\int_0^t \rho_0(\sigma)m(\sigma)\left[\int_\tau^t v(\sigma)\mathrm{d}\eta + l_0\right]^3 \mathrm{d}\tau, \quad (19)$$

where $\dot{\epsilon}$ is the strain-rate and $M$ is the tangent modulus for the elastic region which exhibits non-linear behaviour in high polymer solids. Equation 19 is a Voltera-type integral equation with respect to $\sigma$. Since the strain-rate dependence of $M$ is very small, the next relation of $M$ to $\sigma$ is used for all the strain-rate ranges tested;

$$M = -4.826\sigma + 85.24 \quad (\mathrm{kg\,mm^{-2}}). \quad (20)$$

Calculations of Equation 19 was carried out using the experimental constants given in Sections 4.1 and 4.2, the modulus $M$ being obtained from the stress–strain curves tested in air, as mentioned above.

The solid curves in Fig. 5 show the calculated values obtained at different strain-rates. Comparison between the theoretical and experimental curves indicates that there is quantitative difference at a high strain rate of $0.2\,\mathrm{min^{-1}}$. At a high strain-rate, the craze growth rate in the high stress range, which we were unable to measure in static tension because of the low yield point, is expected to be much lower than the values given by Equation 6, since the high density of crazes causes interaction between individual crazes. However, since this effect is not taken into account in the theory, the computed yield point will be lower than the experimental one. Examination of the specimen surfaces tested at high strain-rates ($2.0\,\mathrm{min^{-1}}$) have shown that the yielding is caused by both crazing and shearing, and the craze yield point is not so

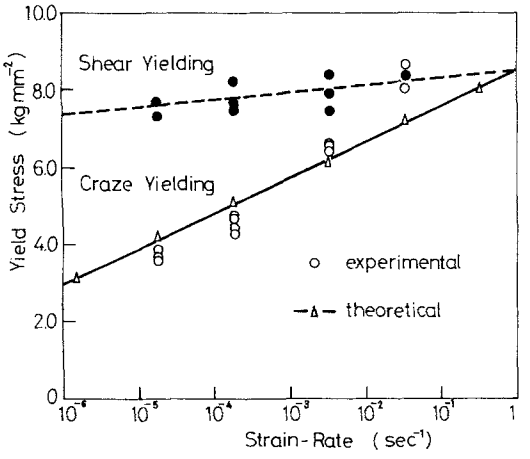


*Figure 7* Effect of strain-rate on craze and shear yield points.

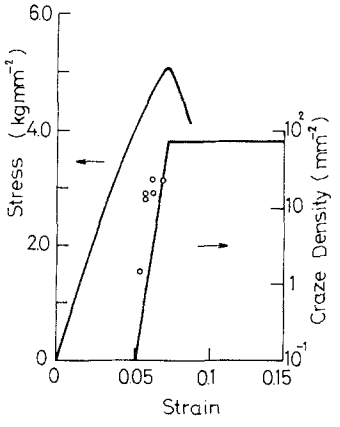


*Figure 8* Comparison of theoretical (———) and experimental (○) variations of craze density with time at a strain-rate of 0.011 $min^{-1}$ in simple tension. The stress–strain curve is theoretical.

different from the shear yield point as indicated in Fig. 7. Therefore, the present theory may not be applied to high strain-rate yielding. Equation 6 may also be applied to the growth rate during yield drop, but the interactions between the crazes and the decreasing stress will make the growth rate smaller than the values expected from Equation 6. Thus, the calculated extent of the yield drop is considered to be greater than that in the experiment. Therefore, an exact description of the craze growth rate is required to understand the yield drop behaviour. Except for the results of high strain-rate tension, the theory agrees well with the experimental data.

Fig. 7 shows the theoretical and experimental strain-rate dependence of the craze yield point. It is found that the craze yield point is more sensitive to strain-rate than the shear yield point. This is characteristic of craze yielding. Although the theory coincides with the experimental data in low strain-rate range, it departs considerably from the experimental results in the high strain-rate range. This departure may suggest a limitation of the application of the present theory to high strain-rate yielding.

Fig. 8 shows the theoretical dependence of craze density on strain at a strain-rate of 0.011 $min^{-1}$. The open circles are in good agreement with the theory. Both the theory and the experiment show that the craze density increases abruptly with increasing strain until yielding occurs. According to the theory, the density in simple tension can be approximated as a function of applied stress in a stress range lower than the yield point by

$$\rho = C \exp(\delta\sigma) \qquad (21)$$

where $\delta$ is a constant and $C$ the strain-rate dependent parameter. Equation 21 is inconsistent with Brown's experimental expression given by a linear function of $\sigma$.

Finally, the theoretical stress relaxation curves are estimated from Equation 7 and 18, and compared with the experimental results. Again it should be noted that the stress is time-dependent. Since the total strain is held constant during the test, the left-hand side of Equation 7 is constant. The computations were performed in the same way as those for the stress–strain curves mentioned above. For the calculations, however, the relaxation modulus in air was used in place of the tangent modulus. The result is shown in Fig. 6. Comparison of the theoretical curve with the experimental ones shows that there are considerable departures from what could be considered to be a good fit. These departures probably result from under-estimation of the craze growth rate at a decreasing stress stage. The experiment, performed by removing the applied stress in a step-like manner, revealed that the craze growth rate is greatly affected by the stress history. Therefore, the exact calculation for the stress relaxation curve may require investigation of craze behaviour under such conditions.

## 5. Conclusions

A theory expressing craze plastic deformations is presented on the basis of a dislocation analogue method extended by Brown, and compared with

the experiments under the conditions of creep, simple tension and stress relaxation. Fairly good agreement between theory and experimental results shows that the dislocation analogue approach is valuable for describing the craze plastic deformation. However, further investigation will be required for an exact description of craze yielding and stress relaxation.

## References


1. J. HOARE and D. HULL, *Phil. Mag.* **26** (1972) 443.
2. N. BROWN *J. Polymer Sci. A-2* **11** (1973) 2099.
3. W.G. JOHNSON and J.J. GILMAN, *J. Appl. Phys.* **30** (1959) 129.
4. N. BROWN, *Phil. Mag.* **32** (1975) 1041.
5. A. S. ARGON and J. G. HANNOOSH, *ibid.* **36** (1977) 1195.
6. A. S. ARGON and M. M. SALAMA, *ibid.* **36** (1977) 1217.
7. I. NARISAWA and T. KONDO, *J. Soc. Sci. Japan* **21** (1972) 321.
8. M. KITAGAWA and M. KAWAGOE *ibid.* **27** (1978) 995.
9. M. I. BESSONOV and E. V. KUVSHINSKY, *Sov. Phys. Solid State* **3** (1961) 950.
10. J. G. WILLIAMS and G. P. MARSHALL, "Deformation and Fracture of High Polymers", edited by H. H. Kausch, J. A. Hassell and R. I. Jaffee (Plenum Press, New York, London, 1974) pp. 557.


Received 20 June and accepted 22 August 1978.